NDT&E International 33 (2000) 401–407

NDT&E international

www.elsevier.com/locate/ndteint

On the study of elastic wave scattering and Rayleigh wave velocity measurement of concrete with steel bar

T.-T. Wu*, J.-H. Sun, J.-H. Tong

Institute of Applied Mechanics, National Taiwan University, Taipei, Taiwan, ROC

Received 21 March 1999; received in revised form 21 January 2000; accepted 3 February 2000

Abstract

This paper presents results on a study of the Rayleigh wave scattering and Rayleigh wave velocity measurement in concrete with a steel bar using transient elastic waves. To study the characteristics of the scattered waves induced by a steel bar in concrete, a three-dimensional heterogeneous finite difference formulation with staggered grids was adopted. The cases for both elastic wave propagation parallel and perpendicular to the steel bar are discussed. The effect of the cover thickness and steel bar spacing on the Rayleigh wave velocity measurement was studied. To confirm the numerical investigations, a concrete specimen containing steel bar was made and the corresponding transient elastic wave experiments were conducted. The numerical results are in good accordance with those of the measured. We note that the result of this study can serve as an important reference in the Rayleigh wave velocity measurement of concrete with steel bar.

Keywords: Transient elastic wave; Concrete; Scattering; Reinforcement

1. Introduction

In the field of nondestructive evaluation, the ultrasonic pulse velocity (longitudinal wave velocity) of concrete specimen has been utilized to predict the strength of concrete in the literature [1,2]. Experimental observations have showed that the pulse velocity is related to the strength of concrete with a reasonable accuracy. On the other hand, the conventional measurements of the elastic properties of concrete specimen are concentrated mostly on the Young's modulus or the longitudinal wave velocity, the shear modulus or the transverse wave velocity are usually not included. Recently, Wu et al. [3,4] proposed a method for determining the dynamic elastic properties of plain concrete specimens using transient elastic waves. In the method, the Rayleigh wave velocity was determined based on the cross correlation method, while the longitudinal wave velocity was determined by measuring the longitudinal wave-front arrival. The wave-front of the longitudinal wave was identified from the tangential component of the surface response directly. With that method, the concrete dynamic elastic properties can be determined through a single transient elastic wave experiment with the utilization of a pair of horizontally polarized conical transducers.

In this paper, the influence of the steel bar on the transient elastic wave propagation and thence on the Rayleigh wave velocity measurement of concrete with steel bar is examined. To study the characteristics of the scattered waves induced by a steel bar in concrete, a three-dimensional heterogeneous finite difference formulation with staggered grids was adopted. The cases for both the elastic wave propagation parallel and perpendicular to the steel bar are discussed. The effects of the cover thickness and steel bar spacing on the Rayleigh wave velocity measurement were studied and discussed. To confirm the numerical investigations, a concrete specimen with steel bar was made and the corresponding transient elastic wave experiments were conducted.

2. Elastic waves in heterogeneous media

For a body with dynamic disturbance propagating in a three-dimensional space, the stress equations of motion can be written in Voigt's form as

$$\rho \frac{\partial v_i}{\partial t} = T_{ij,j} + f_i, \tag{1}$$

where, ρ is the mass density, f_i the body force per unit mass,

* Corresponding author. Tel.: + 886-2-2363-0979; fax: + 886-2-2363-9290.

E-mail address: wutt@spring.iam.ntu.edu.tw (T.-T. Wu).

0963-8695/00/$ - see front matter
PII: S0963-8695(00)00012-8

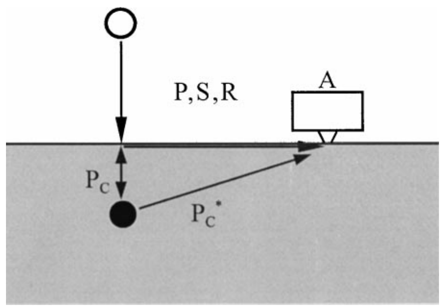

Fig. 1. The wave paths and the testing configuration (the source–receiver line is perpendicular to the axial direction of the steel bar).

T_{ij} the stress components, v_i the particle velocities and $i, j = 1, 2, 3$. For a linear elastic isotropic medium, Hooke's law can be expressed as

$$\frac{\partial T_{ij}}{\partial t} = \lambda v_{k,k} \delta_{ij} + \mu (v_{i,j} + v_{j,i}), \tag{2}$$

where λ and μ are Lamè constants.

A three-dimensional heterogeneous finite difference formulation [5,6] with staggered grids was adopted to study the impact induced transient elastic wave propagation in concrete with steel reinforcement. In this formulation, instead of treating the internal interfaces by explicit interfacial boundary condition, variation of the elastic constants and mass density were employed. The finite difference formulas for interior grid points, surface grid points were derived based on the staggered grid arrangement utilized by Virieux and Madariaga [7], where the traction free surface condition was assumed. Details of the finite difference formulae for the interior as well as the surface grids can be found in Ref. [6]. In this arrangement, either the velocity components or the stress components were defined at different grid. Further, the velocity components and stress components were located at different marching steps. With this arrangement, the numerical stability of the finite difference scheme had been shown unaffected by the value of Poisson's ratio [7]. Therefore, this formulation can be utilized to simulate liquid–solid or air–solid interfaces without further modifications.

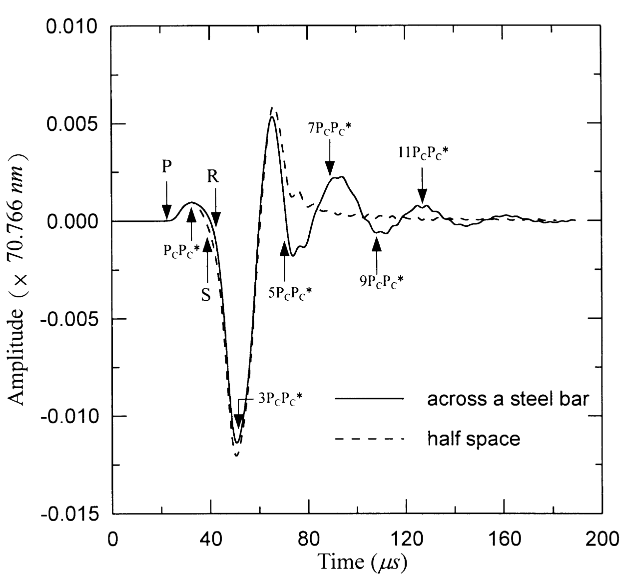

Fig. 2. The tangential component of the displacement signal received at the surface receiver for the testing configuration of Fig. 1. The diameter of the steel bar is 2 cm and the cover thickness is 4 cm ($r_1 = 20$ cm, $T_C = 25$ μs).

In this paper, the aforementioned finite difference method was adopted to simulate the case of three-dimensional propagation of transient elastic waves in concrete with steel bar. In this study, the concrete is assumed to be an isotropic linearly elastic medium. In addition, under the assumption of large wavelength to aggregate size ratio, the concrete is taken as homogeneous. The density, the longitudinal and the transverse wave velocities of the steel bar were assumed as 7850 kg/m^3, 5920 m/s and 3230 m/s, respectively, while those of the concrete were assumed as 2380 kg/m^3, 4220 m/s and 2500 m/s.

3. Scattering of elastic wave by a single steel bar

As shown in Fig. 1, the source–receiver line (the line which connects the impact source and the receiver) is perpendicular to the axial direction of the steel bar. The received wave signal consists of the skimming longitudinal (P) and transverse (S) waves, the Rayleigh surface wave (R), and those waves that are scattered by the steel bar. Depending on the diameter of the steel bar, there is a certain amount of wave energy bouncing back and forth between the impact surface and the steel bar (P_C). For every bouncing wave that hits the steel bar, there is some wave energy scattered out to the receiver (P_C^*) and received by the receiver on the surface.

The solid line in Fig. 2 is the tangential component (parallel to the surface) of the displacement signal received at the surface receiver for the testing configuration of Fig. 1. The source function of the single force utilized in the all the numerical examples is assumed as a half $\sin^{3/2} t$ function with 10 N in magnitude. The distance between the source and the receiver is $r_1 = 10$ cm and the contact duration of the steel ball T_C is assumed as 25 μs. The diameter of the steel bar is 2 cm and the concrete cover thickness (the distance between the concrete surface and the top of the steel bar) is 4 cm. The arrival time of the longitudinal wave, the transverse wave, the Rayleigh wave, and the scattered waves are shown with arrows in the figure. The scattered wave $3P_CP_C^*$ denotes the longitudinal wave which travels three times of the cover thickness and then scatters away from the steel bar to the receiver, and similarly for the symbols of $5P_CP_C^*$. The dashed line shown in Fig. 2 represents the half space response of the same testing configuration without the steel bar. In the half space response, the wave signal after the Rayleigh wave decays gradually to zero. However, the presence of a steel bar in concrete results in a clear oscillation after the Rayleigh wave. It is observed

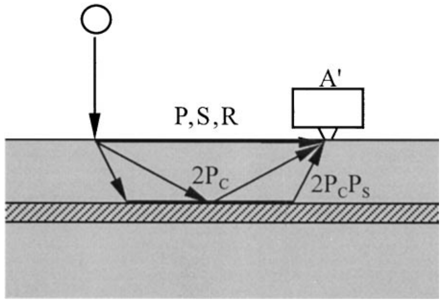

Fig. 3. The wave paths and the testing configuration (the source–receiver line is parallel to the axial direction of the steel bar).

that the arrivals of the scattered waves $3P_CP_C^*$, $5P_CP_C^*$, $7P_CP_C^*$, $9P_CP_C^*$, $11P_CP_C^*$ coincide only approximately with the maximum or minimum of the oscillation after the Rayleigh wave.

For the source–receiver line parallel to the axial direction of the steel bar, in addition to the skimming longitudinal, the transverse, and the Rayleigh surface waves, the received wave signals include the reflected ($2P_C$) and refracted ($2P_CP_S$) waves from the steel bar (Fig. 3). Since, the wave speeds of the steel bar are greater than those of the concrete, at some distance away from the source, the refracted wave ($2P_CP_S$) may arrive earlier than the direct longitudinal wave.

Fig. 4 shows the tangential component (parallel to the surface) of the displacement signal received at the surface receiver for the testing configuration of Fig. 3. The source function, the impact duration, the source to receiver distance, and the cover thickness are all the same as those used in the previous sub-section. The dashed line shown in Fig. 4 represents the half space response of the same testing configuration without the steel bar. The arrival times of the longitudinal wave, the transverse wave, the Rayleigh wave, the reflected and the refracted waves are shown with arrows in the figure. The results in Fig. 4 show that the amplitude of the wave signal oscillation after the Rayleigh wave is smaller than that of wave propagating perpendicular to the steel bar (Fig. 2).

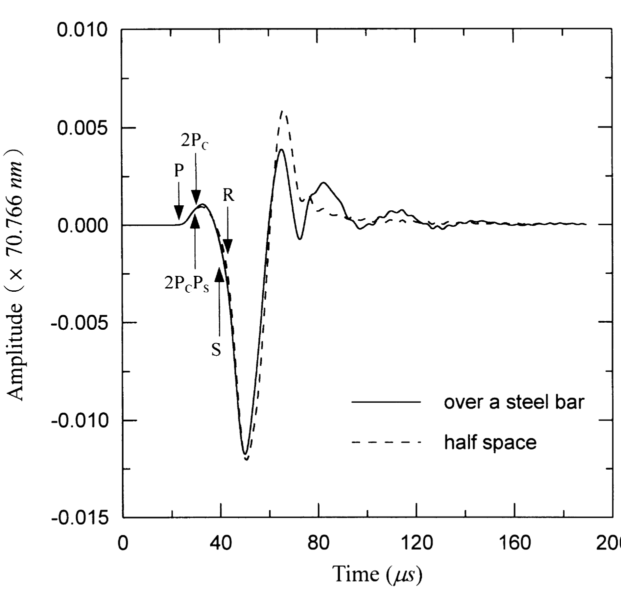

Fig. 4. The tangential component of the displacement signal received at the surface receiver for the testing configuration of Fig. 3. The diameter of the steel bar is 2 cm and the cover thickness is 4 cm ($r_1 = 20$ cm, $T_C = 25$ μs).

4. Effects of cover thickness and steel bar spacing

Since the diameter of the most frequently used steel ball in the impact test is about 5 mm and the associated impact duration is about 25 μs, in the following studies, the impact duration will be fixed at this value for simplicity. To understand the influence of cover thickness and bar spacing on the Rayleigh wave velocity measurement of concrete, a series of numerical simulations were performed.

In the study of the cover thickness effect, one steel bar with diameter of 2 cm was placed in the concrete half space. The figures shown in Fig. 5 are the tangential component of the displacement signals on the surface with the cover thickness varied from 2 to 12 cm at an interval of 2 cm. In the testing configuration, the source–receivers line is right on top of the steel bar and along its axial direction. The distance between the impact source and the first receiver is 10 cm and that between the first receiver and the second receiver is also 10 cm. The solid line in the figures represents the signals recorded at the first receiver (10 cm) and the dashed line represents the signals at the second receiver (20 cm). From close look on the figures in Fig. 5, we note that the smaller the cover thickness, the bigger the influence of the scattering effect of the steel bar on the wave signals. As the cover thickness is large enough (compared with the wavelength of the Rayleigh wave), the influence of the steel bar can be neglected. For example, one can find that in Fig. 5, these signals with cover thickness larger than 10 cm are similar to that of a half space.

To understand the effect of the steel bar spacing *W* on the scattering of impact induced elastic waves in a concrete half space with multiple parallel steel bars, a series of numerical simulations were performed. In the simulations, the impact duration was fixed at 25 μ*s*, the cover thickness and the diameter of the steel bars were assumed as 4 and 2 cm, respectively. The spacing of the steel bars were varied from 4 to 12 cm at an interval of 2 cm. As shown in Fig. 6, the source–receivers line is along the axial direction of the steel bars and is directly above the steel bar. The signals shown in Fig. 6 are the tangential component of the waves recorded at the first receiver (10 cm) and second receiver (20 cm), respectively. The results show that the scattered (reflected) signals from the adjacent steel bars are added together, and then, make the signal oscillation after the Rayleigh wave last longer than that for the case of a single steel bar. The amplitude of the long oscillation decreases as the spacing of the steel bars is increased. We note that when the spacing reaches 12 cm in this simulation, the wave

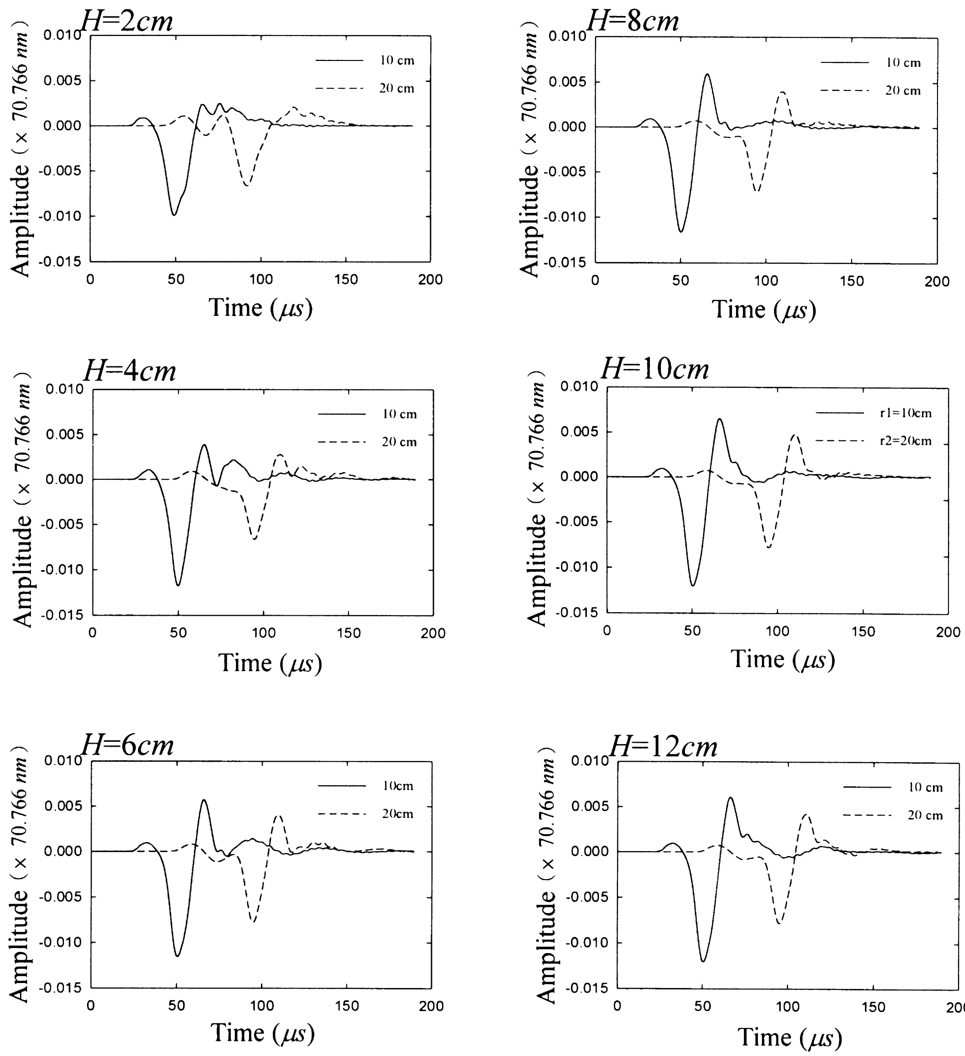

Fig. 5. The tangential component of the displacement signals on the surface with the cover thickness varied from 2 to 12 cm at an interval of 2 cm ($r_1 = 10$ cm, $d = 10$ cm, $T_C = 25$ μs).

signal is similar to that of the single steel bar case (Fig. 5, $H = 4$ cm).

5. Rayleigh wave velocity measurement

The theoretical background for measuring the in-situ elastic wave velocities of plain concrete has been given by Wu et al. [3] and Wu and Fang [4]. In the measurement of Rayleigh wave velocity using transient elastic waves, two receivers (S_1 and S_2) are employed. The distance between the source and the first receiver S_1 is r_1, and the distance between the first and second receiver S_2 is d. In order to utilize the cross correlation method to determine the Rayleigh wave transit time between the first receiver and the second receiver, it is required that the distance r_1 must be large enough to ensure that the Rayleigh wave carries most of the energy. Letting $h_1(t)$ and $h_2(t)$ be the signals recorded at S_1 and S_2, respectively, the cross correlation function of these two signals is defined as

$$z(t) = \int_{-\infty}^{\infty} h_1(t) h_2(t + \tau)\, d\tau \tag{3}$$

If the similar signals $h_1(t)$ and $h_2(t)$ are separated by a time delay Δt, the maximum of $z(t)$ occurs at $t = \Delta t$. In other words, the time delay between $h_1(t)$ and $h_2(t)$ can be determined by finding the corresponding time at which $z(t)$ is maximum. Once the time delay is determined, the Rayleigh wave velocity can be obtained by dividing the travel distance with the time delay.

According to previous study [4], we note that the calculated Rayleigh wave velocity based on the correlation method is almost equal to the exact Rayleigh wave velocity as the nondimensional distance r_1^* between the source and the first receiver is large enough. The nondimensional distance was defined as $r_1^* = r_1/(C_R T_C)$ with C_R the exact Rayleigh wave velocity and T_C the impact duration.

In the previous section, we studied the scattering effect of

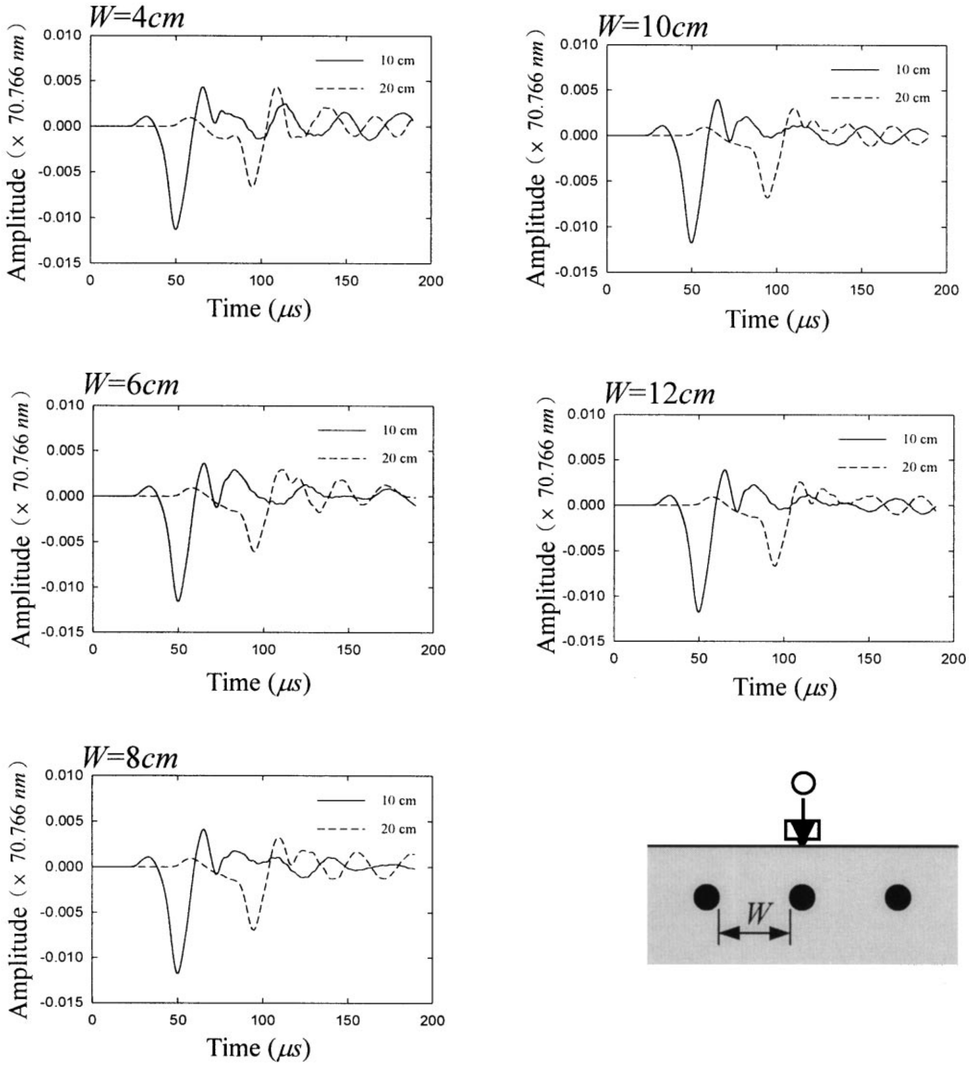

Fig. 6. The effect of steel bar spacing on the tangential component of the surface responses. The spacing of the steel bars were varied from 4 to 12 cm at an interval of 2 cm ($r_1 = 10$ cm, $d = 10$ cm, $T_C = 25$ μs, $H = 4$ cm).

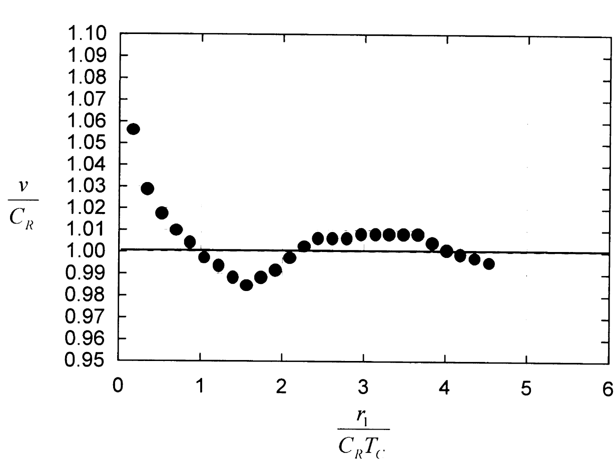

Fig. 7. Numerical simulation of the influence of r_1^* on the Rayleigh wave velocity measurements in plain concrete.

a steel bar in concrete and realized that the scattered wave signals mainly appeared after the arrival of the Rayleigh wave spike. In this section, we are going to investigate the influences of steel bar and the bar spacing on the Rayleigh wave velocity measurement when the correlation method is invoked. For comparison with the results of Rayleigh wave velocity measurement in concrete with steel bar, the numerical simulation of the influence of r_1^* on the Rayleigh wave velocity measurements in plain concrete were conducted first and is shown in Fig. 7. The vertical axis is the ratio of the calculated (v) and the true Rayleigh wave velocity (C_R).

To understand the influences of cover thickness (H) on the Rayleigh wave velocity measurement, the numerical signals shown in Fig. 5 were processed and the results are shown in Fig. 8. From the results, we note that as the cover thickness is smaller than 4 cm, the determined Rayleigh wave velocities are about two or three percent higher than the true Rayleigh wave velocity of the concrete. For H

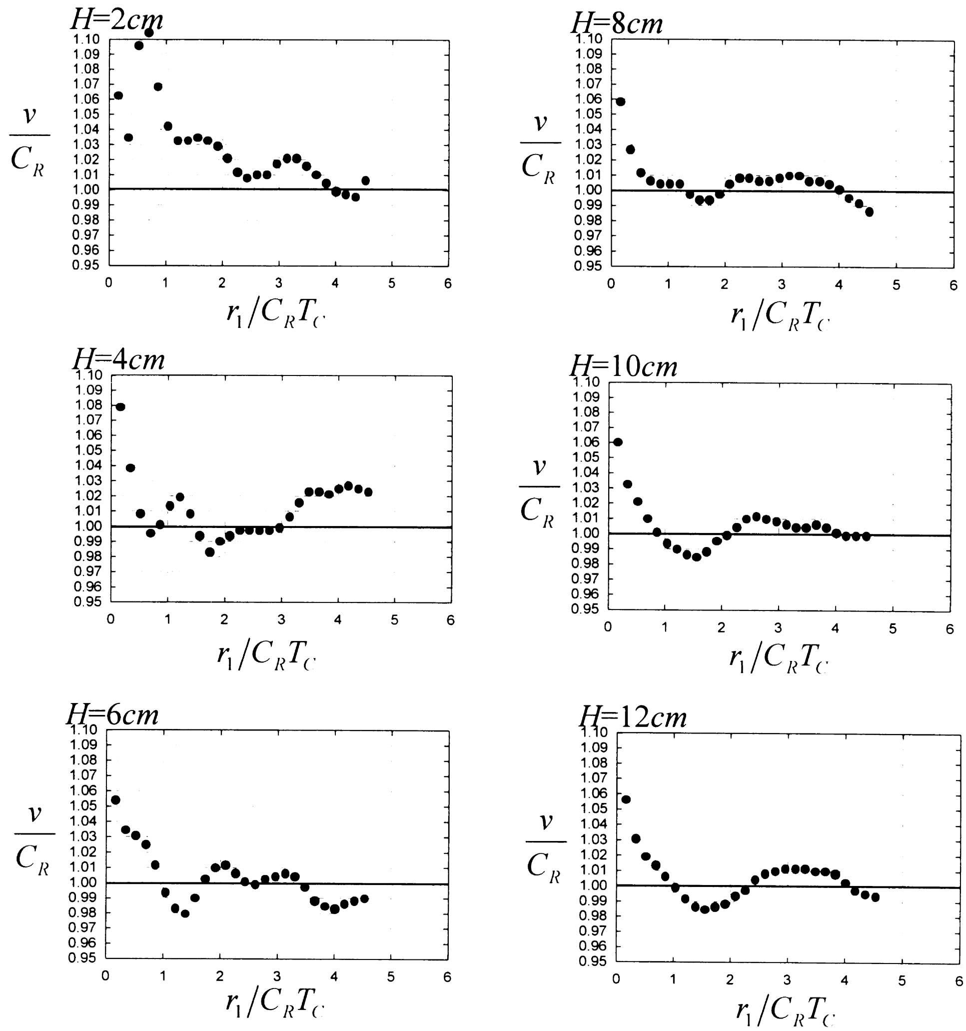

Fig. 8. The influences of r_1^* on the Rayleigh wave velocity measurements for different cover thickness H.

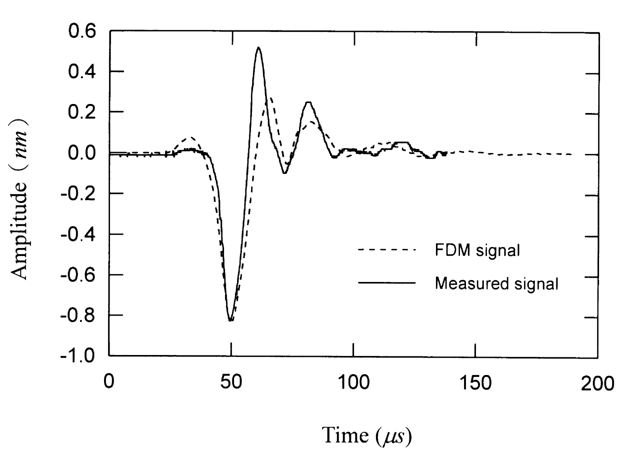

Fig. 9. The measured tangential component of the displacement signal received at the surface receiver (the same testing configuration as Fig. 3, $r_1 = 10$ cm, $T_C = 25$ μs, $H = 4$ cm).

greater than or equal to 4 cm, the values of the calculated Rayleigh wave velocities oscillate around the true value of the Rayleigh wave velocity. On the other hand, as the cover thickness increases to 8 cm, we note that the results are similar to those calculated for a concrete half space (Fig. 7). This confirms that the energy of Rayleigh surface wave is concentrated mostly within the surface layer of one to two wavelengths.

Studies on the effects of the steel bar spacing were performed and similar characteristics were observed. The results show that the calculated Rayleigh wave velocities are oscillated up and down around the true value C_R as r_1^* varied. As the spacing W is getting larger, the effect of the spacing on the calculated Rayleigh wave velocity is getting smaller.

6. Experimental confirmation

In this paper, a concrete specimen consisting of a single

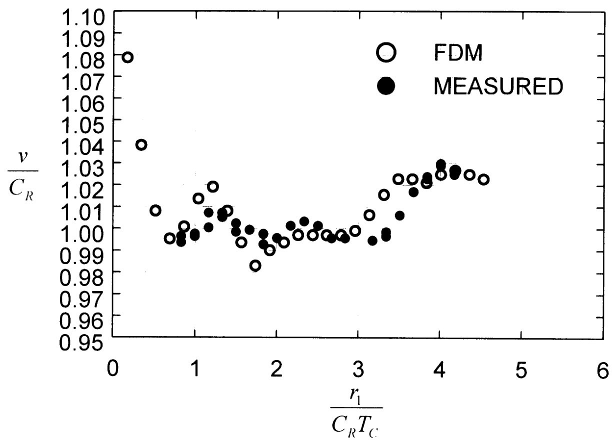

Fig. 10. The Rayleigh velocity measurements with different r_1^*.

steel bar of 2 cm in diameter and 4 cm in cover thickness was made. The dimensions of the concrete specimen were 60 cm by 60 cm with 30 cm in thickness. In the Rayleigh wave velocity measurements, two homemade horizontally polarized conical transducers were utilized to measure the tangential component of the surface displacement signals. The received voltage signals from the conical transducers were amplified by preamplifiers and recorded by a 100MHz digital oscilloscope (LeCroy 9314L). A steel ball with a 4.75 mm diameter was used as the impact source and the corresponding impact duration was approximately 25 μs.

Fig. 9 shows the calculated (dashed line) and the measured (solid line) tangential component (parallel to the surface) of the displacement signal received at the surface receiver on the specimen (the same testing configuration as Fig. 3). The impact source to the receiver distance was 10 cm. The time origin of the measured signal is arbitrary. Since the force of the steel impact was not measured, the unit of the measured signal is arbitrary. Comparing the calculated and the measured signals, we note that the experimentally observed signal oscillation after the Rayleigh wave is the same as predicted. Although, there is some deviation between the calculated and the measured signals, the general characteristics of the scattering waves from the steel bar is predicted by the numerical calculation with good accuracy. Shown in Fig. 10 are the associated Rayleigh velocity measurements of the specimen as a function of r_1^*. The solid circles represent those based on the measured signals, and open circles represent the simulated result (the same as Fig. 8, $H = 4$ cm). We note that the measured results are in good agreement with those predicted by the numerical simulation.

7. Conclusion

In this paper, we studied the elastic wave scattering in a concrete specimen with steel bar, and further, examined its influence on the Rayleigh wave velocity measurement using transient elastic waves. Both the cases for waves propagating parallel and normal to the steel bar were examined. The results showed that the presence of steel bar scattered the wave causing an oscillatory signal amended after the Rayleigh wave spike. Results on the studies of the cover thickness and steel bar spacing on the Rayleigh wave velocity measurement showed that if the cover thickness or the spacing is relatively large, the influence of the reinforcement on the Rayleigh wave velocity measurement is negligible. To confirm the numerical investigations, a concrete specimen with a steel bar embedded was made and the corresponding transient elastic wave experiments were conducted. The experimental results were in agreement with the numerical predictions.

Acknowledgements

The authors thank the financial support of this research from the National Science Council of ROC (NSC87-2211-E-002-062).

References

[1] Standard Test Method for Pulse Velocity Through Concrete, ASTMC597-71, 1979.
[2] Ben-Zeitun AE. Use of pulse velocity to predict compressive strength of concrete. Int J Cement Composites Light Weight Concrete 1986;8(1):51–59.
[3] Wu T-T, Fang J-S, Liu G-Y, Kuo M-K. Determination of elastic constants of a concrete specimen using transient elastic waves. J Acoust Soc Am 1995;98(4):2142–8.
[4] Wu T-T, Fang J-S. New method for measuring concrete elastic constants using horizontally polarized conical transducers. J Acoust Soc Am 1997;101(1):330–6.
[5] Wu T-T, Fang J-S. Inverse determination of surface-breaking cracks in concrete using transient elastic waves. Part I: numerical forward simulation. J Chin Inst Civil Hydraulic Engng 1997;9(4):627–36.
[6] Fang J-S, Wu T-T. Inverse determination of surface-breaking cracks in concrete using transient elastic waves. Part II: experiment and inversion. J Chin Inst Civil Hydraulic Engng 1997;9(4):637–46.
[7] Virieux J, Madariaga R. Dynamic faulting studied by a finite difference method. Bull Seism Soc Am 1982;72:345–69.